We are IntechOpen, the world's leading publisher of Open Access books Built by scientists, for scientists

4,800
Open access books available

122,000
International authors and editors

135M
Downloads

Our authors are among the

154
Countries delivered to

TOP 1%
most cited scientists

12.2%
Contributors from top 500 universities

CLARIVATE ANALYTICS BOOK CITATION INDEX INDEXED

WEB OF SCIENCE™

Selection of our books indexed in the Book Citation Index in Web of Science™ Core Collection (BKCI)

Interested in publishing with us?
Contact book.department@intechopen.com

Numbers displayed above are based on latest data collected.
For more information visit www.intechopen.com

10

A Fast Method to Compute Radiation Fields of Shaped Reflector Antennas by FFT

Abolghasem Zeidaabadi Nezhad[1], Zaker Hossein Firouzeh[2] and Hamid Mirmohammad-Sadeghi[2]
[1]*Department of Electrical & Computer Engineering, Isfahan University of Technology*
[2]*Information and Communication Technology Institute (ICTI)*
IRAN

1. Introduction

Interest in reflector antennas due to attractive features including high gain, multiple beam, low side lobe level, and robustness have been growth both in military and commercial areas in microwave frequency range since World War I. In particular, low side lobe level radiation pattern, is an essential requirement for satellite communication systems. Offset reflector antennas featuring adjacent high gain beams with good isolation across the same frequency bandwidth make them good candidates for these applications. Depending on the required radiation pattern, feeds may or may not be located at the focus. A cluster of feeds can be used in the focal region of offset reflectors for multiple beams application [Skolnik, 1990; Chu and Turrin, 1973; Rudge, 1975; Janken et al., 1973; Ingerson and Wong, 1974; Tian et al., 2007].

There have been published lots of articles dealing with analyze and design of electrically small and large reflectors by analytical or numerical techniques [Love, 1978; Wood, 1986; Lo and Lee, 1988; Scott, 1990]. These methods vary from the traditional Aperture Field Method (AFM) that involves integrating the electric fields scattered by the reflector onto a projected planar aperture, to more modern hybrid methods that employ a variety of techniques each of which is applicable over different regions of the radiation pattern. Some of the aforementioned methods yield exact solutions such as, Method of Moments (MoM) but require significantly computational resources. Larger reflectors like large radio astronomy antennas need to be analysed using high-frequency techniques which use approximations based on asymptotic solutions for canonical problems. The approximate techniques have been proved to be quite successful in predicting both far and near-field patterns and are in very good agreement with the measurements. Methods of evaluating the electromagnetic fields radiated from a reflector antenna fall into two categories: exact and approximation methods. These various techniques have been explained as follows [Philips et al., 1996].

The Method of Moments is the most accurate technique in all known methods used in electromagnetic scattering analysis. The formulation of the governing equations of the problem (such as Electric Field Integral Equation (EFIE)) is exact, and highly accurate solutions can be obtained by a suitable choice of basis and testing functions. The induced

current distribution on the reflector surface is obtained by MoM to calculate the electromagnetic scattering fields. The Method of Moments is well documented in the literature providing classical textbooks that describe the technique [Harrington, 1993; Moore and Pizer, 1984; Miller et al., 1992]. Using this approach, one can accurately evaluate the full radiation properties of any antenna by wire grid [Popovic et al., 1982] or patch model [Wilton & Butler, 1981]. Additionally, the antenna can be analyzed in free space or infinite dielectric half plane. The main drawback of this method is the large computational resources required. Therefore, the MoM is not a practical approach for antennas larger than a few wavelengths. Recently, Wavelet-Based Moment Method (WBMM) has been applied on large reflector antennas to calculate the current distribution accurately and fast. By serving wavelets as basis and testing functions in a wavelet expansion, a sparse matrix is generated from the previous MoM dense matrix, which may save computational cost. By use of this method, the currents on the reflector surface can be calculated faster than the conventional MoM [Lashab et al., 2007; Lashab et al., 2008; Herzberg, 2005].

Approximation methods or high frequency methods can be applied on electrically large antennas to predict far-field and near-field radiation characteristics [Rusch and Potter, 1970; Kauffman et al., 1976]. These methods are subdivided into three types; those based on the Kirchoff's approximation (such as Aperture Field Method, Scalar Radiation Integral/Projected Aperture Method, Physical Optics (PO), Gaussian Beam Mode optics (GBM)), Ray tracing methods (such as Geometrical Optics (GO), Geometrical or Uniform Theory of Diffraction (GTD/UTD)), and also corrected Kirchoff's methods (such as Physical Optics and Physical Theory of Diffraction (PTD)) [Philips et al., 1996]. The high frequency methods are well suited for the analysis of electrically large reflector antennas as well as for the modelling of secondary effects such as the interaction of the main antenna with adjacent structures similar to building or terrain obstacles.

Methods based on Kirchoff's approximation are utilized generally for the estimation of the antenna boresight, main lobe and few adjacent sidelobes. Aperture field method and projected aperture method fail to predict the cross polar pattern with sufficient degree of accuracy [Silver, 1949]. In addition, the minimum radii of curvature should be more than five wavelengths in size for validity of Geometrical Optics [Philips et al., 1996]. The most widely used method is Physical Optics which involves the vector summation of radiated fields due to individual currents induced over the structure by the illuminating fields which have been evaluated by considering the Geometrical Optics propagation due to the primary feed [Balanis, 1989]. In terms of CPU time and storage requirements, the Aperture Field Method or projected aperture method is significantly more efficient than Physical Optics. However, PO is generally more accurate than the former and correctly predicts the main beam and close in sidelobes. It also gives a better prediction of the cross polar pattern.

Methods based on the Kirchoff's approximation suffer from the inability to provide accurate predictions at angles widely displaced from the antenna's main beam direction. Although the computational requirements for the summation of the Physical Optics current are not as severe as in the case of the MoM, it is nevertheless a significant factor to consider taking into account that the sampling interval on the reflector surface needs to be of the order of a wavelength or less [Philips et al., 1996].

An alternative fast analytical way for evaluating the radiative properties of the antenna is the Gaussian Beam Mode (GBM) analysis [Goldsmith, 1982; Lamb, 1986; Bogush and Elgin, 1986; Lesurf, 1990]. The Gaussian beam mode fields are given by simple analytical

expressions; hence this formulation offers advantages due to the simplicity and the speed of evaluation. The analysis is valid in both the near and the far-field points along the paraxial directions with equally rapid and straightforward evaluations. Furthermore, the expansions are valid in the transition regions. However, GBM cannot predict the far-out sidelobe region and blockage due to subreflector or struts which should be either negligible or avoided for valid results.

The wide angle and non-paraxial direction can be predicted by a ray description of the diffracted field. This is accomplished with the introduction of diffracted rays within the framework of Geometrical Theory of Diffraction [Keller, 1958; Keller, 1962], or its uniform versions such as the Uniform Theory of Diffraction [Kouyoumjian and Pathak, 1974] and Uniform Asymptotic Theory (UAT) [Ahluwalia et al., 1968], which provides diffracted field expressions valid across the shadow boundaries of the incident or reflected fields. The diffraction coefficients contain Fresnel integrals that are easily evaluated, thus providing a fast and efficient algorithm for the analysis of large reflectors. Most of the time is actually used in locating the points of reflection and diffraction on the reflector, given the source and field points. With multiple reflectors and complex geometrical shapes, this can sometimes be quite time-consuming although not nearly as much as in evaluating double integrals over large surfaces. It must be emphasised that any ray description fails at caustics and so a purely ray technique cannot predict the far-field characteristics of a large antenna near boresight. Such regions can be analysed by the Equivalent Current Method (ECM) [Ryan and Peters, 1969], which works back from the GTD solution away from caustics to obtain an equivalent current that would produce identical fields there. This current is then used to extrapolate the field at the caustics.

A PO plus UTD scheme may well be the first option for evaluating the radiated field from a large reflector antenna. The PO is used to predict the radiation characteristics in the boresight region and the UTD to evaluate the wide angle characteristics of the radiation pattern. Prediction of the antenna backlobe can be calculated by defining an equivalent edge current using the basic UTD formulation. This current is integrated in the usual far-field sense to provide the radiation pattern in the rearward direction. The implementation of a UTD scheme offers significant speed enhancement combined with minimal memory requirements. The GO plus UTD combination can also provide very rapid field calculations, but fails to predict the main beam characteristics. However, it can be used to provide full near-field predictions [Philips et al., 1996].

The problem of wide angle and non-paraxial direction prediction can be solved when the Physical Optics method is augmented with Physical Theory of Diffraction (PTD), which is a systematic extension of the PO approach, just as GTD is an extension to GO [Ufimtsev, 2007]. The PTD correction consists of a fringe current acting along the rim of the quasi-optical system. The value of these fringe currents is such that the edge condition is satisfied; hence the diffraction phenomenon is accurately described. The PO plus PTD scheme can provide accurate near and far-field information along any direction. However, this method when applied to electrically large systems may require large amounts of memory and computer time due to evaluation of surface and line integration.

After choosing the proper method to analyze the desired reflector antenna, the speed and the accuracy of the radiation pattern computation of the reflector antennas is very important. The most straightforward as well as the most time-consuming method is the direct numerical quadrature of the radiation integral for the aperture antenna. Several

approaches have been proposed for the efficient numerical evaluation of the double radiation integrals. The earliest of these is the so-called Ludwig algorithm in which the double integral can be evaluated in explicit closed forms [Ludwig, 1968; Ludwig, 1988]. Alternatively, one can expand the radiation integral into a series such as the one in the Jacobi-Bessel method [Rahmat-Samii et al., 1980; Galindo-Israel and Mittra, 1977]. The Jacobi-Bessel method is most suited for computing the pattern of antennas which have a circular projected aperture. Because the Jacobi polynomials satisfy a special type of recursion relationship, they are also useful for computing the radiation pattern of parabolic reflector antennas. Another approach to the secondary pattern computation of planar or parabolic antennas has been suggested by Drabowitch [Drabowitch, 1965]. This approach is based on the two-dimensional sampling theorem. The coefficients of the interpolating functions for the secondary pattern are computed by periodically sampling the secondary pattern at intervals determined by the aperture dimensions. These coefficients are subsequently used in conjunction with the interpolating functions to compute the secondary pattern at an arbitrary observation angle.

In this chapter, an algorithm is presented to evaluate aperture numerical integration by FFT method. This coordinate system is used for all antenna configurations. The proposed algorithm can be applied to all shaped reflector antennas which has been illuminated by defocused feeds with arbitrary patterns. In this method, in order to calculate the radiation patterns, the equations of geometrical optics are used to calculate the reflected electric field using the radiation patterns of the feed and the parameters defining the reflector surface. In addition, the direction of the reflected ray and the point of intersection of the reflected ray with the aperture plane are obtained by use of geometrical optics. These fields comprise the aperture field distribution which is integrated over the aperture plane by FFT to yield the far-field radiation pattern and to calculate other antenna parameters. Shaped Reflector Antenna Design and Analysis Software (SRADAS) based on this numerical method can analyze and simulate all shaped reflector antennas with large dimensions in regard to the wavelength. SRADAS has been implemented and used in Information and Communication Technology Institute (ICTI) to analyze and simulate different practical parabolic and shaped reflector antennas [Zeidaabadi Nezhad and Firouzeh, 2005].

The organization of this chapter is as follows: Proposed fast method to calculate the radiation integral of a parabolic reflector antenna is explained in Section 2. Required mesh size in order to accomplish the optimum mesh density in calculating the radiation integrals with desired accuracy and speed is introduced in section 3. In order to confirm the validity of the proposed calculation method, in Sections 4 and 5, two types of practical antennas are analyzed by this method and the results are compared with the results achieved by the commercial software package FEKO and measurements, as well. Finally, concluding remarks are given in Section 6.

2. Calculation of the radiation integrals by FFT

Fig. 1 shows the three-dimensional geometry of a parabolic reflector antenna. A feed located at the focal point of a parabola forms a beam parallel to the focal axis. In addition, the rays emanating from the focus of the reflector are transformed into plane waves. The design is based on optical techniques, and it does not take into account any diffraction from the rim of the reflector. Since a parabolic antenna is a parabola of revolution, the equation (1) describes

the parabolic surface in terms of the spherical coordinates r', θ', ϕ', where f is the focal distance. Because of its rotational symmetry, there are no variations with respect to ϕ'. The projected cross-sectional area of reflector on the aperture plane -the opening of the reflector- is S_0, and on the focal plane is S_0'.

$$r' = \frac{2f}{1+\cos\theta'} = f \sec^2\left(\frac{\theta'}{2}\right) \quad \theta' \le \theta_0 \tag{1}$$

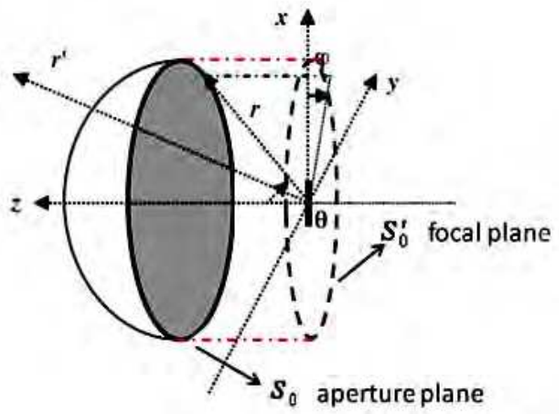

Fig. 1. Three-dimensional geometry of a parabolic reflector antenna

The total pattern of the system is computed by the sum of secondary field and the primary field of the feed element. For the majority of feeds like horn antennas, the primary pattern in the boresight direction of the reflector is of very low intensity and usually can be neglected.
The advantage of the AFM is that, the integration over the aperture plane can be performed easily for any feed position and any feed pattern, whereas the double integration on current distribution over the reflector surface is time-consuming in PO method, and it becomes difficult when the feed is placed off-axis or when the feed radiation pattern has no symmetry.
The radiation integrals over S_0' computing the far fields by AFM can be written as [Balanis, 2005]:

$$E_{\theta S} = \frac{j\beta e^{-j\beta r}}{4\pi r}(1-\cos\theta)\iint_{S_0'}\left(-E_{ax}\cos\phi - E_{ay}\sin\phi\right) \exp(j\beta\left(x'\sin\theta\cos\phi + y'\sin\theta\sin\phi\right))\,dx'dy' \tag{2a}$$

$$E_{\phi S} = \frac{j\beta e^{-j\beta r}}{4\pi r}(1-\cos\theta)\iint_{S_0'}\left(-E_{ax}\sin\phi + E_{ay}\cos\phi\right) \exp(j\beta\left(x'\sin\theta\cos\phi + y'\sin\theta\sin\phi\right))dx'dy' \tag{2b}$$

$$\beta = \frac{2\pi}{\lambda} \quad , \quad u = \sin\theta\cos\phi \quad v = \sin\theta\sin\phi \tag{2c}$$

In equations (2), $E_{\alpha x}$ and $E_{\alpha y}$ represent the x- and y-component of the reflected fields over S_0'. The spherical coordinates of the observation point is r,θ,ϕ. λ and β are wavelength and phase constant of the propagated wave in free space, respectively.

A feed at the focal point of a parabola forms a beam parallel to the focal axis. Therefore, the only difference between fields on S_0 and S_0' is the constant phase because of the distance between the aperture plane S_0 and the focal plane S_0'. Additional feeds displaced from the focal point form multiple beams at angles off the antenna axis. In this case, the reflected fields from the reflector are not parallel to the focal axis resulting in a severe phase distortion between fields on S_0 and S_0'. Therefore, the integral equations (2a) and (2b) are calculated over the aperture plane S_0, not the focal plane S_0'. The phase distortion increases with the angular displacement in beamwidths and decreases with an increase in the focal length.

In order to calculate the reflected filed from the reflector, a rectangular mesh is created on the focal plane S_0' as shown in Fig. 2. According to AFM and GO, the reflected fields out of S_0' are vanished. Two-dimensional FFT is used to compute the integral equations (2a) and (2b) rapidly [Bracewell, 1986]. Integrals P_X and P_Y are defined as:

$$\begin{aligned} P_x &= \iint_{S_0'} E_{\alpha x}\ e^{j\beta\left(x'u+y'v\right)}\,dx'dy' \\ P_y &= \iint_{S_0'} E_{\alpha y}\ e^{j\beta\left(x'u+y'v\right)}\,dx'dy' \end{aligned} \tag{3}$$

Using the equations of (3), radiation fields $E_{\theta S}$ and $E_{\phi S}$ can be calculated by:

$$\begin{aligned} E_{\theta S} &= \frac{j\beta e^{-j\beta r}}{4\pi r}\left(1-\cos\theta\right)\left\{-P_x\cos\phi - P_y\sin\phi\right\} \\ E_{\phi S} &= \frac{j\beta e^{-j\beta r}}{4\pi r}\left(1-\cos\theta\right)\left\{-P_x\sin\phi + P_y\cos\phi\right\} \end{aligned} \tag{4}$$

The mesh grid is generated by the following expressions:

$$\begin{aligned} \Delta x' &= \frac{d}{M-1}\ ,\ x' = -\frac{d}{2} + m.\Delta x'\ ,\ m = 0,1,2,...,M-1 \\ \Delta y' &= \frac{d}{N-1}\ ,\ y' = -\frac{d}{2} + n.\Delta y'\ ,\ n = 0,1,2,...,N-1 \end{aligned} \tag{5}$$

Where, M and N are the number of points which have been distributed uniformly in x- and y-direction of S_0' plane. The aperture diameter of the parabolic reflector is d. The relations of (3) and (5) lead to:

$$\begin{aligned} P_x &= \exp\left(-j\beta u\frac{d}{2}\right)\exp\left(-j\beta v\frac{d}{2}\right)\Delta x'\Delta y'\sum_{m=0}^{M-1}\sum_{n=0}^{N-1}E_{\alpha x}\left(m,n\right)e^{j\beta v\frac{nd}{N-1}}\,e^{j\beta u\frac{md}{M-1}} \\ P_y &= \exp\left(-j\beta u\frac{d}{2}\right)\exp\left(-j\beta v\frac{d}{2}\right)\Delta x'\Delta y'\sum_{m=0}^{M-1}\sum_{n=0}^{N-1}E_{\alpha y}\left(m,n\right)e^{j\beta v\frac{nd}{N-1}}\,e^{j\beta u\frac{md}{M-1}} \end{aligned} \tag{6}$$

$E_{ax}(m,n)$ and $E_{ay}(m,n)$ are the electric fields at the mesh points (m,n) of S_0' plane. Comparison between the equations of (6) with FFT formulas, the angles of spherical coordinate of far-field radiation electric fields, θ_{kl} and ϕ_{kl} are calculated using the following expressions:

$$\begin{aligned} A &= \frac{d}{\lambda}\frac{M}{M-1} \quad , \quad k = -A\sin\theta_{kl}\cos\phi_{kl} \quad , \quad k = 0,1,2,...,M-1 \\ B &= \frac{d}{\lambda}\frac{N}{N-1} \quad , \quad l = -B\sin\theta_{kl}\sin\phi_{kl} \quad , \quad l = 0,1,2,...,N-1 \end{aligned} \tag{7a}$$

$$0 \le \theta_{kl} \le \pi \ , \ 0 \le \phi_{kl} \le 2\pi \ \ or \ \ -\pi \le \phi_{kl} \le \pi$$

$$\begin{aligned} \theta_{kl} &= \sin^{-1}\left(\left[\left(\frac{k}{-A}\right)^2 + \left(\frac{l}{-B}\right)^2\right]^{1/2}\right) \\ \phi_{kl} &= \tan^{-1}\left(\frac{-Al}{-Bk}\right) \end{aligned} \tag{7b}$$

Two-dimensional FFT (FFT2) formulas can be used to rewrite the relations of (6), that is:

$$\begin{aligned} P_x &= \exp\left(-j\beta u\frac{d}{2}\right)\exp\left(-j\beta v\frac{d}{2}\right)\Delta x'\Delta y'\,FFT\,2\left(E_{ax}\right) \\ P_y &= \exp\left(-j\beta u\frac{d}{2}\right)\exp\left(-j\beta v\frac{d}{2}\right)\Delta x'\Delta y'\,FFT\,2\left(E_{ay}\right) \end{aligned} \tag{8}$$

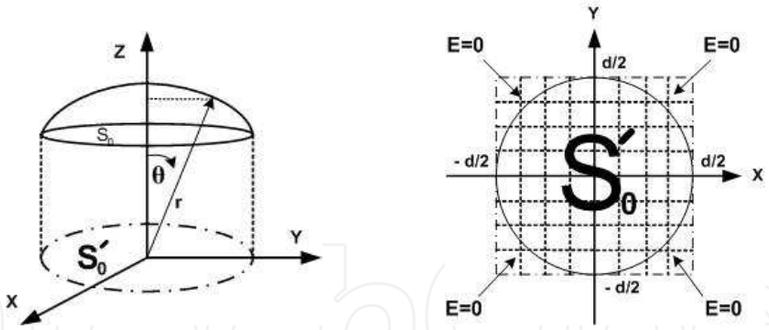

(a) (b)

Fig. 2. (a) Plane S_0' is the projected cross-sectional area of reflector on the focal plane. (b) A rectangular mesh is created on the plane S_0'. d is the aperture diameter of the parabolic reflector.

Finally, radiation fields of $E_{\theta S}$ and $E_{\phi S}$ are computed by using FFT2. It can be written as:

$$\begin{aligned} E_{\theta S} &= \frac{j\beta e^{-j\beta r}}{4\pi r}\left(1-\cos\theta_{kl}\right)\left\{-\cos\phi_{kl}P_x - \sin\phi_{kl}P_y\right\} \\ E_{\phi S} &= \frac{j\beta e^{-j\beta r}}{4\pi r}\left(1-\cos\theta_{kl}\right)\left\{-\sin\phi_{kl}P_x + \cos\phi_{kl}P_y\right\} \end{aligned} \tag{9}$$

Based on the equations (8) and (9), far fields of $E_{\theta S}$ and $E_{\phi S}$ are calculated, where θ_{kl} are the angles calculated by (7). Negative values of l and k are used to find the fields in other regions. In addition, number of main points of the major lobe found by FFT is constrained. Therefore, it is interpolated from above points to obtain E- and H-planes Half-Power beamwidths (HP_E and HP_H). The principal E- and H-plane radiation patterns can be calculated by substituting $\phi = \pi/2$ and $\phi = 0$, respectively. According to [Stutzman and Thiele, 1981], directivity D can be calculated as:

$$D = \frac{4\pi}{\Omega_A}$$
$$\Omega_A = \iint_{u^2+v^2 \le 1} \left| F(u,v) \right|^2 \frac{dudv}{\sqrt{1-u^2-v^2}} \tag{10}$$

Ω_A is the antenna beam solid angle. $F(u,v)$ is the radiation pattern of the reflector antenna in terms of the variables u and v. The main equations are prepared to analyze a paraboloidal reflector and to compute the radiation characteristics. Moreover, SRADAS can be applied to all shaped reflector antennas with defocused feed elements provided that dimensions of the reflector are large in regard to the wavelength.

3. Calculation of the optimum mesh size

In general, if x(t) is a continuous function of t in the interval of [a ,b], Fourier transform pair of x(t) can be written as the following [Bracewell, 1986]:

$$x(t) = \int_{-\infty}^{+\infty} X(f) e^{+j2\pi ft} df \tag{11a}$$

$$X(f) = \int_{-\infty}^{+\infty} x(t) e^{-j2\pi ft} dt \tag{11b}$$

To calculate the Fourier integrals numerically, the interval of [a, b] is divided into N-1 segments uniformly by use of N points. The step size ΔT is:

$$\Delta T = \frac{b-a}{N-1}$$
$$t = a + n\Delta T \quad , \quad n = 0,1,2,...,N-1 \tag{12}$$

After substitution of (12) in the Fourier transform pair, (11b) can be estimated using the following expression:

$$X(f) \approx \sum_{n=0}^{N-1} x[n] e^{-j\frac{2\pi}{N} f \frac{n(b-a)N}{(N-1)}} \tag{13}$$

By comparison (13) to Discrete Fourier Transform, it can be written as:

$$X(k)=\sum_{n=0}^{N-1}x[n]e^{-j\frac{2\pi}{N}kn} \qquad k=0,1,2,...,N-1$$
$$k=N\Delta Tf \Rightarrow f_k=\frac{k}{N\Delta T}\Rightarrow f_{\max}=\frac{N-1}{N\Delta T} \tag{14}$$

Where, ΔT should be less than $\frac{N-1}{N}\frac{1}{f_{\max}}$ until the maximum frequency component of x(t) can be detected by Discrete Fourier Transform. Since N is very large, the preceding relation can be reduced as:

$$\Delta T \le \frac{1}{f_{\max}} \tag{15}$$

It is obvious that the radiation integrals are the spatial Fourier Transform of the aperture electric fields. Therefore, f_x and f_y are the spatial frequencies corresponding to x and y axes, respectively. The mesh size should satisfy the following relation based on (15):

$$\Delta x<\frac{1}{f_x},\ f_x=\frac{u}{\lambda}\Rightarrow \Delta x<\frac{\lambda}{u},\ \ Max(u)=1\Rightarrow \Delta x<\lambda \tag{16}$$

Similarly, it can be proved that $\Delta y<\lambda$. As a result, the mesh size should be less than λ until the aperture electric fields can be sampled correctly to compute the radiation integrals numerically by FFT accurately. Near-field measurement in the case of planar scanning shows the sampling interval is better to choose $\lambda/2$ or less to have more accurate phase detection [Philips et al., 1996].

In this section, in order to evaluate the effect of mesh size in calculating the radiation pattern, a typical parabolic reflector antenna excited by a feed horn has been simulated. The operating frequency of the antenna is 1.3 GHz. The diameter and the focal distance are 13.5m and 5.31m, respectively. Simulated results for different mesh sizes by SRADAS have been shown in Table 1. For mesh size greater than λ=23.08cm, the antenna parameters such as Gain and Half Power (HP) beamwidths are not accurate. However, when the mesh size is less than λ, the condition (16) is satisfied, and the radiation characteristics will be calculated correctly. When mesh points of M=128 and N=128 are chosen, the main beam is at the angle of θ=180° and the Gain is 38.91dB. HP beamwidths are 2.34° in the E-plane radiation pattern and 0.9° in the H-plane radiation pattern. Calculated side lobe levels are -35dB and -25dB in E-plane and H-plane, respectively. E-plane and H-plane radiation patterns have been depicted in Fig. 3.

In order to validate the proposed calculation method the parabolic reflector antenna has been simulated by FEKO software. FEKO results have been given in Table 2. As it can be noticed there are some discrepancies between the proposed analytical method and FEKO result. The first reason is that, for simplicity, diffraction effects have been ignored in calculation in SRADAS. Also, the interpolation method has been used to compute both of Gain and HP beamwidths. However, the consumed time of simulation by SRADAS is about one-third of FEKO simulation time. The calculation speed of SRADAS is faster than the simulation performed for the same structure by FEKO software and both results are in good agreement.

In the following sections, to evaluate the proposed calculation method, SRADAS, antenna parameters of two practical radar antennas are calculated and the results are compared both with FEKO and measurements.

M	N	dx (cm)	dy (cm)	Main beam θ (deg.)	HP_E^o	HP_H^o	Gain (dB)
32	32	43.55	43.55	180	62.89	32.42	11.06
48	48	28.72	28.72	180	24.62	14.12	18.73
56	56	24.55	24.55	180	5.24	2.32	33.30
64	64	21.47	21.47	180	2.34	0.9	38.83
100	100	13.64	13.64	180	2.34	0.9	38.90
128	128	10.63	10.63	180	2.34	0.9	38.91

Table 1. Simulated results for different meshing sizes by SRADAS

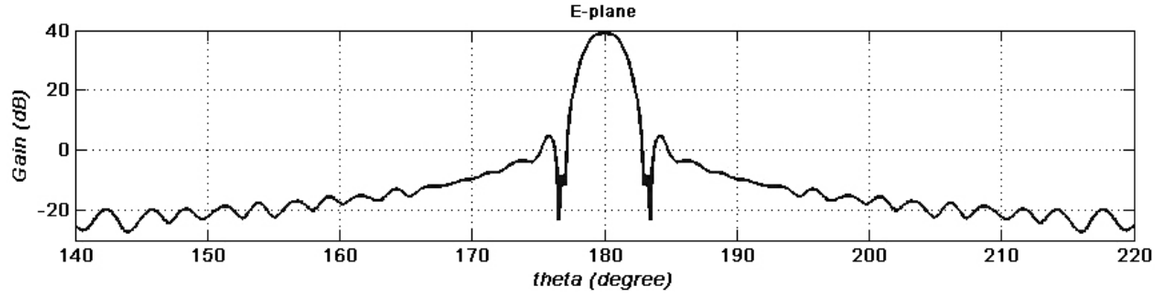

(a)

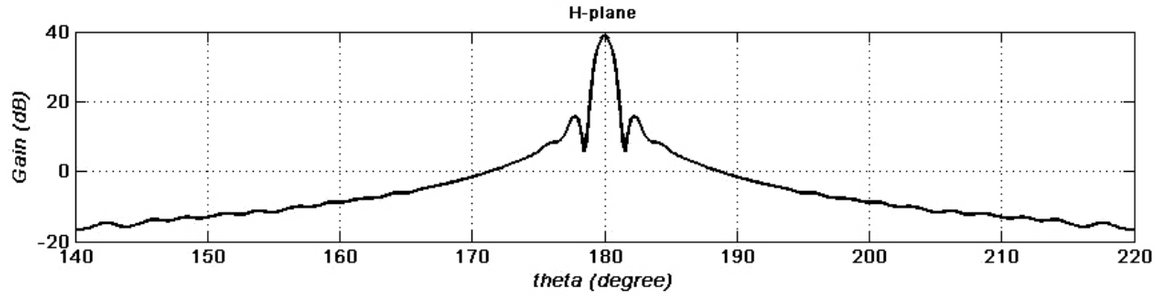

(b)

Fig. 3. (a) E-plane radiation pattern (b) H-plane radiation pattern

	Main beam θ (deg.)	HP_H^o	HP_E^o	Gain (dB)	SLL_E (dB)	SLL_H (dB)
SRADAS	180	2.34	0.9	38.91	-35	-25
FEKO	180	2.5	1.1	39.2	-33	-22

Table 2. Comparison radiation characteristics simulated by FEKO software and SRADAS

4. Analysis of a shaped reflector antenna illuminated by two displaced feed horns

A shaped reflector antenna fed by two displaced feed horns (Fig. 4) has been simulated by SRADAS. The operating frequency of the antenna is 1.4 GHz. Reflector aperture is 7.0m in height and 13.5m in width with a focal axis of 5.31m. The profile of azimuth curve is parabola and the profile of elevation curve is an unusual function. The 3-dimensional

mathematical function which determines the reflector surface of the antenna is obtained by curve fitting method as:

$$z = -0.0471x^2 + 5.3100\cos^{0.6364}\left(\frac{y}{4.9267}\right) \tag{17}$$

The feed horns have been placed in y-direction symmetrically in relation to the origin. The feed horn which has been located in (0, 0,-0.185m) radiates the higher beam and the other one located in (0, 0, 0.185m) radiates lower one.
Simulated results by SRADAS have been shown in Table 3. Both of M and N for meshing the reflector aperture are 128. Results provided by FEKO have been given in Table 4. Because of large dimensions, radiation patterns of the antenna have been measured using outdoor far-field measurement method (open-site method). The gain of higher beam is 35.5dB and that of lower one is 34.5dB. Azimuth HP beamwidth ($HP_H°$) is 1.2° and elevation HP beamwidth ($HP_E°$) is about 10.5°. The results obtained for this antenna using presented numerical method are in good agreement with both measurements and FEKO software. The consumed time of simulation by SRADAS is about one-third of the time consumed by FEKO.

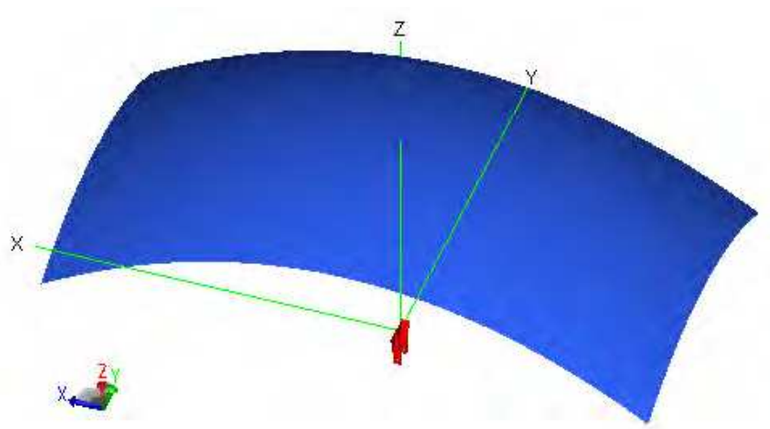

Fig. 4. A shaped reflector antenna illuminated by two horns

Beam	Y (m)	Elevation (deg.)	Azimuth (deg.)	Gain (dB)	$HP_E°$	$HP_H°$	SLL_E (dB)	SLL_H (dB)
Low	+0.185	-1.85	+90	34.1	11.1	1.0	-40	-35
High	-0.185	+1.85	+90	34.1	11.1	1.0	-40	-35

Table 3. Radiation characteristics simulated by SRADAS

Beam	Y (m)	Elevation (deg.)	Azimuth (deg.)	Gain (dB)	$HP_E°$	$HP_{XOZ}°$	SLL_E (dB)	SLL_{XOZ} (dB)
Low	+0.185	-2	+90	33.4	12.2	0.8	-34	-32
High	-0.185	+2	+90	33.4	12.2	0.8	-34	-32

Table 4. Radiation characteristics simulated by FEKO software

5. Simulation of AN/TPS-43 Antenna

The TPS-43 Radar as shown in Fig. 5 is a transportable three-dimensional air search Radar which operates in frequency range of 2.9 to 3.1 GHz with a 200 mile range. The reflector antenna is a paraboloid of revolution with elliptic cross-section from front view. Reflector aperture is 4.27m high by 6.20m wide with focal axis of 2.6m. The reflector is illuminated by 15 horn antennas which has been moved progressively back from the focal plane [Skolnik, 1990]. Feed horn 2 has been located at the focus of the reflector. The feed array features the use of a stripline matrix to form the 6 height-finding beams. Transmitting radiation pattern of Radar is fan beam for surveillance but receiving radiation pattern is stacked beam to detect height of a target.

Using SRADAS software, AN/TPS-43 antenna has been simulated and the results have been shown in Table 5 and Fig. 6. Comparing the results provided by the proposed method in Fig. 6 with results reported by M. L. Skolnik [Skolnik, 1990] for this antenna confirm the integrity of SRADAS. Some discrepancies can be noticed between them, those are, because of that the locations of feed horns of available Radar are a little different from Radar in reference [Skolnik, 1990]. In addition, diffraction effects have been neglected by use of SRADAS. The calculation speed of SRADAS is so faster than the simulation performed for the same structure by FEKO software and both results are in good agreement.

Fig. 5. AN/TPS-43 Antenna

	Elevation (deg.)	Azimuth (deg.)	Gain (dB)	HP_E (deg.)	HP_H (deg.)
Beam 1	0	0	39.05	1.80	0.9
Beam 2	4.32	90	38.12	1.98	0.9
Beam 3	7.15	90	37.06	1.98	0.9
Beam 4	12.30	90	36.10	3.78	0.9
Beam 5	17.50	90	35.03	4.30	0.9
Beam 6	23.40	90	31.20	5.22	1.26

Table 5. Radiation characteristics of final 6 beams of TPS-43 Radar simulated by SRADAS

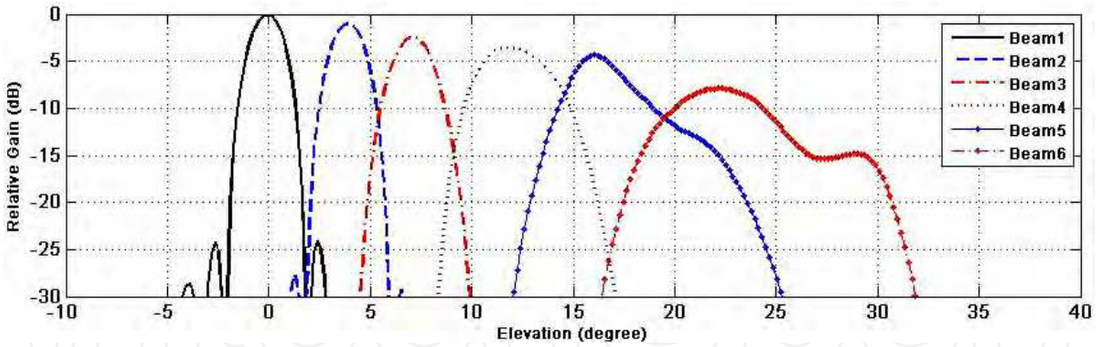

Fig. 6. Elevation radiation patterns of TPS-43 Radar simulated by SRADAS

6. Conclusion

The development and application of a numerical technique for the rapid calculation of the far-field radiation patterns of a reflector antenna excited by defocused feeds have been reported. The reflector has been analyzed by Aperture Field Method (AFM) and Geometrical Optics (GO) to predict the radiation fields in which the radiation integrals computed by FFT. The analytical and numerical results demonstrate that the maximum mesh size of the aperture plane should be less than a wavelength to compute the radiation integrals accurately. Developed Shaped Reflector Antenna Design and Analysis Software (SRADAS) based on MATLAB applied for two practical Radar antennas shows that SRADAS can be used for all shaped reflector antennas with large dimensions compared to operating wavelength. SRADAS has been implemented and used in Information and Communication Technology Institute (ICTI) to analyze and simulate different practical parabolic and shaped reflector antennas. Not only SRADAS has a library of conventional reflectors, but also is it possible to define the geometry of the desired reflector. In addition, SRADAS has the ability to simulate all of shaped reflector antennas fed by defocused feeds rapidly with good accuracy in comparison with available commercial software FEKO. The consuming simulation time performed by SRADAS is less than that of simulated by FEKO software. Consequently, SRADAS can be used as an elementary tool to evaluate the designed reflector antenna in regard to achieving the most important radiation characteristics of the reflector antenna. After that, more accurate simulation can be down by complicated and time-consuming electromagnetic softwares such as FEKO or NEC.

7. Acknowledgment

The authors would like to thank the staff of Information and Communication Technology Institute (ICTI), Isfahan University of Technology (IUT), Islamic Republic of Iran for their co-operator and supporting this work.

8. References

Ahluwalia, D. S.; Lewis, R. M. & Boersma, J. (1968). Uniform asymptotic theory of diffraction by a plane screen, *SIAM Jour. Appl. Math.*, Vol. 16, No. 4, 783-807, 0063-1399

Balanis, C. A. (1989). *Advanced Engineering Electromagnetics,* John Wiley & Sons, 0471621943, New York

Balanis, C. A. (2005). *Antenna Theory, Analysis and Design*, 3rd ed., John Wiley & Sons, 047166782X, New York

Bogush, A. & Elgin, T. (1986). Gaussian field expansion for large aperture antennas, *IEEE Trans. Antennas & Propagation*, Vol. 34, No. 2, 228-243, 0018-926X

Love, A. W. (1978). *Reflector Antennas*, John Wiley & Sons, 0471046051, New York

Bracewell, R. N. (1986). *The Fourier Transform and Its Applications*, McGraw-Hill, 0070070156, New York

Chu, T. S. & Turrin, R. H. (1973). Depolarization properties of offset reflector antennas. *IEEE Trans. Antennas & Propagation*, Vol. 21, No. 3, 339-345, 0018-926X

Drabowitch, S. (1965). Application aux antennas de la theorie du signal. *L'Onde Electrique*, Vol. LXIV, No. 458, 550-560

Galindo-Israel, V. & Mittra, R. (1977). A new series representation for the radiation integral with application to reflector antennas. *IEEE Trans. Antennas & Propagation*, Vol. 25, No. 5, 631-641, 0018-926X

Goldsmith, P. F. (1982). Quasi-optical techniques at millimeter and sub-millimeter wavelengths, In: *Millimeter and Infrared Waves*, Vol. 6, Button, K. J. (Ed.), 277-343, Academic Press, 0121477126, New York

Harrington, R. F. (1993). *Field Computation by Moment Methods*, IEEE Press, 0780310144, New York

Herzberg, T.; Ramer, R. & Hay, S. (2005). Antenna analysis using wavelet representations, *Progress In Electromagnetics Research Symposium*, pp. 48-52, Hangzhou, China, Aug. 2005

Ingerson, P. G. & Wong, W. C. (1974). Focal region characteristics of offset fed reflectors, *IEEE/Antennas and Propagation Society International Symposium*, pp. 121-123, Jun. 1974

Janken, J. A.; English, W. J. & DiFonzo, D. F. (1973). Radiation from multimode reflector antennas, *IEEE/Antennas and Propagation Society International Symposium*, pp. 306-309, Aug. 1973

Kauffman, J. F.; Croswell, W. F. & Jowers, L. J. (1976). Analysis of the radiation patterns of reflector antennas. *IEEE Trans. Antennas & Propagation*, Vol. 24, No. 1, 53-65, 0018-926X

Keller, J.B. (1958). A geometric theory of diffraction, In: *Calculus of Variations and its Applications*, *Proceedings of Symposia in Applied Math, Vol. 8*, Graves, L. M. (Ed.), McGraw-Hill Book Company Inc., New York

Keller, J. B. (1962). Geometrical theory of diffraction, *Jour. Opt. Soc. Amer.*, Vol. 52, No. 2, 116-130, 1084-7529

Kouyoumjian, R.G. & Pathak, P. H. (1974). A uniform geometrical theory of diffraction for an edge in a perfectly conducting surface. *Proceedings of the IEEE*, Vol. 62, No. 11, 1448-1461, 0018-9219

Lashab, M.; Benabdelaziz, F. & Zebiri, C. (2007). Analysis of electromagnetic scattering from reflector and cylindrical antennas using wavelet-based moment method. *Progress In Electromagnetics Research*, Vol. 76, 357–368, 1070-4698

Lashab, M.; Zebiri, C. & Benabdelaziz, F. (2008). Wavelet-based moment method and physical optics use on large reflector antennas. *Progress In Electromagnetics Research M*, Vol. 2, 189–200, 1937-8726

Lamb, J. W. (1986). Quasi-optical coupling of gaussian beam systems to large cassegrain antennas, *Int. Jour. Infrared Millimeter Waves*, Vol. 7, 1511-1536, 0195-9271

Lesurf, J. C. G. (1990). *Millimetre-wave Optics Devices and Systems*, Adam Hilger, 0852741294, Bristol

Lo, Y. T. & Lee, S. W. (1988). *Antenna Handbook: Theory, Applications, and Design*, Van Nostrand Reinhold Co., 0442258437, New York

Ludwig, A. C. (1968). Computation of radiation patterns involving numerical double integration, IEEE Trans. Antennas & Propagation, Vol. 16, No. 6, 767-769, 0018-926X

Ludwig, A. C. (1988). Comments on the accuracy of the Ludwig integration algorithm, *IEEE Trans. Antennas & Propagation,* Vol. 36, No. 4, 578-579, 0018-926X

Miller, E. K.; Medgyesi-Mitschang, L. & Newman, E. H. (1992). *Computational Electro-Magnetics: Frequency Domain Method of Moments*, IEEE Press, 0879422769, New York

Moore, J. & Pizer, R. (1984). *Moment Methods in Electromagnetics: Techniques and Applications*, Research Studies Press, 0863800130, Letchworth

Philips, B.; Philippakis, M.; Philippou, G. Y. & Brain, D. J. (1996). *Study of Modelling Methods for Large Reflector Antennas,* Radio Communications Agency, London

Popovic, B. D.; Dragovic, M. B. & Djordjevic, A. R. (1982). *Analysis and Synthesis of Wire Antennas*, Research Studies Press, 0471900087, New York

Rahmat-Samii, Y.; Galindo-Israel, V. & Mittra, R. (1980). A plane-polar approach for far-field construction from near-field measurements. *IEEE Trans. Antennas & Propagation*, Vol. 28, No. 2, 216-230, 0018-926X

Rusch, W. V. T. & Potter, P. D. (1970). *Analysis of Reflector Antennas*, Academic Press, 0126034508, New York

Rudge, A. W. (1975). Multiple-beam antennas: offset reflectors with offset feeds. *IEEE Trans. Antennas & Propagation,* Vol. 23, No. 3, 317-322, 0018-926X

Ryan, C. E. Jr. & Peters, L. Jr. (1969). Evaluation of edge diffracted fields including equivalent currents for caustic regions, IEEE Trans. Antennas & Propagation, Vol. 17, No. 3, 292-299, 0018-926X

Scott, C. (1990). *Modern Methods of Reflector Antenna Analysis and Design,* Artech House, 0890064199, Boston, Mass

Silver, S. (1949). *Microwave Antenna Theory and Design*, MIT Radiation Laboratory Series, Vol. 20, McGraw-Hill, New York

Skolnik, M. I. (1990). *Radar Handbook,* 2nd ed., McGraw-Hill, 007057913X, New York

Stutzman, W. L. & Thiele, G. A. (1981). *Antenna Theory and Design,* John Wiley & Sons, 047104458X, New York

Tian, Y.; Zhang, Y. H. & Fan, Y. (2007). The analysis of mutual coupling between paraboloid antennas. *Jour. of Electromagn. Waves and Appl.*, Vol. 21, No. 9, 1191–1203, 0920-5071

Ufimtsev, P. Ya. (2007). *Fundamentals of the Physical Theory of Diffraction*, John Wiley & Sons, 047009771X

Wilton, D. R. & Butler, C. M. (1981). Effective methods for solving integral and integro-differential equations, *Electromagnetics*, Vol. 1, No. 3, 289-308

Wood, P. J. (1986). *Reflector Antenna Analysis and Design*, Peter Peregrinus, 0863410596

Zeidaabadi Nezhad, A. & Firouzeh, Z. H. (2005). *Analysis and Simulation of Shaped Reflector Antennas*, Internal Report at ICTI Library, Isfahan, IRAN

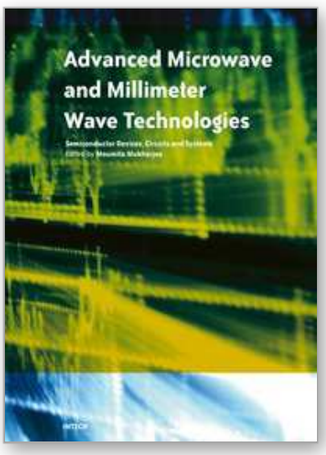

Advanced Microwave and Millimeter Wave Technologies
Semiconductor Devices Circuits and Systems
Edited by Moumita Mukherjee

ISBN 978-953-307-031-5
Hard cover, 642 pages
Publisher InTech
Published online 01, March, 2010
Published in print edition March, 2010

This book is planned to publish with an objective to provide a state-of-the-art reference book in the areas of advanced microwave, MM-Wave and THz devices, antennas and systemtechnologies for microwave communication engineers, Scientists and post-graduate students of electrical and electronics engineering, applied physicists. This reference book is a collection of 30 Chapters characterized in 3 parts: Advanced Microwave and MM-wave devices, integrated microwave and MM-wave circuits and Antennas and advanced microwave computer techniques, focusing on simulation, theories and applications. This book provides a comprehensive overview of the components and devices used in microwave and MM-Wave circuits, including microwave transmission lines, resonators, filters, ferrite devices, solid state devices, transistor oscillators and amplifiers, directional couplers, microstripeline components, microwave detectors, mixers, converters and harmonic generators, and microwave solid-state switches, phase shifters and attenuators. Several applications area also discusses here, like consumer, industrial, biomedical, and chemical applications of microwave technology. It also covers microwave instrumentation and measurement, thermodynamics, and applications in navigation and radio communication.

INTECH
open science | open minds

InTech Europe
University Campus STeP Ri
Slavka Krautzeka 83/A
51000 Rijeka, Croatia
Phone: +385 (51) 770 447
Fax: +385 (51) 686 166

InTech China
Unit 405, Office Block, Hotel Equatorial Shanghai
No.65, Yan An Road (West), Shanghai, 200040, China
中国上海市延安西路65号上海国际贵都大饭店办公楼405单元
Phone: +86-21-62489820
Fax: +86-21-62489821

www.intechopen.com

IntechOpen

IntechOpen